Microchimica Acta (2020) 187:443
https://doi.org/10.1007/s00604-020-04430-4

ORIGINAL PAPER

Fluorescent detection of Cu (II) ions based on DNAzymatic cascaded cyclic amplification

Jingjing Tian[1,2,3] · Zaihui Du[1,2,3] · Longjiao Zhu[1,2,3] · Xiangli Shao[1,2] · Xiangyang Li[4] · Wentao Xu[1,2,3]

Received: 25 February 2020 / Accepted: 7 July 2020

Abstract

A fluorescent biosensor based on the cascaded cyclic amplification-lighted copper nanoparticles has been developed, optimized, and validated. In the double-modular cascaded cyclic amplification, a DNAzymatic cyclic amplification unit transforms metal ion signal to specific DNA sequences, and a linear/exponential integrated amplification unit converts as-prepared DNA codes to identical thymine (T)-rich DNA templates. T-rich scaffolds can induce the generation of red fluorescent copper nanoparticles, with fluorescence emission at 625 nm upon the excitation at 340 nm, as signal vehicles for quantitative detection of metal ions. Copper ions, selected as the model target, could be detected in a wide linear range from 10 to 10^4 nM depending on the increased fluorescent intensity, and the detection limit is 5.6 ± 0.52 nM ($n = 3$) within 40 min, which is 4 orders of magnitude lower than the limits set in drinking water. In the detection of Cu^{2+} in real tap and lake water, the results between inductively coupled plasma mass spectrometry (ICP-MS) and our proposed biosensor were consistent, illustrating the practicability of the fabricated method. In summary, the established fluorescent biosensor compensates the deficiency of immunoassays failing to analyze metal ions, broadens ranges of biomarkers responding to cleaved DNAzymes, provides an open platform sensing different metal ions, and meets the increasing need for the ultrasensitive detection in the field of food safety, environmental monitoring, and medical diagnosis.

Keywords DNA nanotechnology · Copper nanoparticles · Cascaded cyclic amplification · Biosensor

Introduction

Analytical science is intended to detect wide ranges of targets with satisfactory performance [1]. Rapid detection techniques are of great importance for sustainable development and human health [2]. Thereinto, antibody (Ab)-based immunoassays and enzyme-linked immunosorbent assays play a crucial role in detecting diverse targets, such as pesticide residues [3], hormones [4], antibiotics [5], enzymes [6, 7], and even whole cells [8]. However, there are two main contemporary challenges facing the mentioned technique. First, biomarkers difficult to prepare antibodies are hardly detected by immunoassays. Second, detection performances are limited to sensitivity, yet the growing demand for lower detection limit has still to be met in the existing immune formats.

Recently, the booming development of DNA nanotechnology promotes the creation of exquisite DNA nanostructures intelligent to respond to broader range of analytes and the nano-scaled amplification more likely to improve sensitivity [9, 10]. As an identification element, the metal ion or pathogen-dependent DNAzyme, which is a single-stranded DNA with complex tertiary nanostructures by in vitro selection [11], can cleave or ligate DNA substrates with constitutively imperative metal ions or pathogens as cofactors [12–15]. The screening of DNAzymes has greatly expanded ranges of biomarkers. Acting as a signal transformation element, the magnifying effect of DNA amplification, from classical polymerase

Electronic supplementary material The online version of this article (https://doi.org/10.1007/s00604-020-04430-4) contains supplementary material, which is available to authorized users.

✉ Wentao Xu
xuwentao@cau.edu.cn

[1] Key Laboratory of Precision Nutrition and Food Quality, Department of Nutrition and Health, China Agricultural University, Beijing 100083, China

[2] Key Laboratory of Functional Dairy, Ministry of Education, College of Food Science and Nutritional Engineering, China Agricultural University, Beijing 100083, China

[3] Key Laboratory of Safety Assessment of Genetically Modified Organism (Food Safety), Ministry of Agriculture, Beijing 100083, China

[4] Food Science and Engineering College, Beijing University of Agriculture, Beijing 102206, China

chain reaction (PCR) [16, 17] to isothermal amplification [18], improves the detection performance dramatically. Nevertheless, as for an output signal, DNA-based platforms tend to be assisted with labeled molecules, always accompanied by complex operation and increased costs [19].

The compilation, calculation, and templation characteristics make DNA an intriguing biopolymer in signal output [20]. Nowadays, low cost, easy synthesis, and high stability push the progress of DNA nano-engineering forward rapidly [9]. As a representative, DNA-templated noble metal nanoparticles, from gold [21] and silver [22] to copper nanoparticles [23], can be generated in situ and used as a smart stimuli-responsive signal carrier in bioanalytical systems [24, 25]. Particularly, in response to thymine (T)-rich ssDNA or adenine (A)/T-combined dsDNA, copper nano-shaped particles are induced to emit bright red fluorescence with high photostability in an instantaneous synthesis [26, 27]. With its superior fluorescent peculiarity, copper nanoparticles provide an intelligent means for a label-free and ultrasensitive vehicle in the output module of DNA-based biosensors.

Lately, sensors for assays of Hg^{2+} [28], Zn^{2+} [29], Cr^{3+} [30], Pb^{2+} [31, 32], and Mg^{2+} [33, 34] have been established. Especially, Cu^{2+} [35–37] as low as nanomole can be detected selectively. Although their performance has been improved depending on the introduced nanomaterials or interfaces, the preparation step in advance is unavoidable. In our study, fluorescent copper nanoparticles can be produced instantaneously during detection, and the copper ion (II) was selected as the metallic ion-typed model target. Cu^{2+} in low doses often acts as an enzyme cofactor and is indispensable in substance metabolism and energy metabolism; however, excessive exposure to Cu^{2+} from food and the environment can cause diverse detrimental conditions [38]. A fluorescent biosensor based on cascaded cycling DNA amplification-lighted nano-shaped particles was developed. In the presence of Cu^{2+}, cascaded cycling amplification, composed of DNAzymatic cyclic amplification and linear/exponential integrated amplification, was designed to transform ion signals to thymine (T)-rich ssDNA sequences for signal conversion and amplification. Then, fluorescent copper nanoparticles were induced with the guidance of T-rich oligonucleotides in situ within several minutes, and the emitting red fluorescence was monitored by a fluorescent colorimeter with no labeled signal molecules and excellent ultrasensitive and selective performance.

Experiments

Reagents

All DNA sequences, shown in Table 1, were synthesized at Invitrogen (Life Technologies, Beijing, China). Dynabeads® MyOne™ Streptavidin T1 and SYBR Gold nucleic acid gel stain were purchased from Thermo Scientific (Life Technologies, Beijing, China). Deoxythymidine triphosphate (dTTP), dNTPs, Bst DNA polymerase, and nicking endonuclease Nt.Bst NBI were acquired from New England Biolabs (NEB, Beijing, China). 4-(2-Hydroxyethyl)-1-piperazineethanesulfonic acid (HEPES), 3-(4-morpholino) propanesulphonic acid (MOPS), $CuSO_4$, and sodium ascorbate were obtained from Sigma Aldrich Chemical Co. (St. Louis, MO, USA). All other chemicals were of analytical grade and used without further purification. Ultrapure water used in this work was purified by the Millipore water purification system (resistivity ≥ 18.2 M Ω cm^{-1}, Milli-Q).

Instruments

Fluorescent measurements were acquired by means of a Cary Eclipse Fluorimeter (Agilent, USA). Gel electrophoresis was observed on a Molecular Imager Gel Doc XR (Bio-Rad, Canada). Real-time EXPAR analysis was conducted by means of a CFX96 real-time PCR detection system (Bio-Rad, Canada), while the high-resolution transmission electron micrograph (TEM) was performed on a JEM-2100 transmission electron micrograph (JEOL, Germany).

Preparation of DNAzymatic cyclic amplification

To obtain Cu^{2+}-dependent isothermal multiple DNAzymatic cycles, the mixture of 100 nM molecular beacon (MB) substrate and 50 nM enzymatic strand in 50 mM HEPES buffer (pH 7.0) containing 1.5 M NaCl were heated at 95 °C for 2 min and then cooled to room temperature. Until the as-prepared Cu^{2+}-dependent cleaving DNAzymes had formed adequately, they were coupled with Dynabeads via biotin-avidin conjugation (see Supplementary material document). Thereafter, different concentrations of $CuSO_4$ were added to initiate the isothermal multiple DNAzymatic cyclic amplification in the cleaving buffer (1.5 M NaCl, 50 mM HEPES, and 50 μM ascorbate, pH 7.0) at 37 °C. After 20-min cleavage, the cyclic system was separated through magnetism, and the sediment was recycled before the next use.

Preparation of linear-exponential integrated amplification

To avoid nonspecific background amplification, the preparation of 20 μL exponential amplification system was divided into two sections. Section A comprised 0.5 × Nt.BstNBI Reaction Buffer (50 mM Tris-HCl, 100 mM NaCl, 10 mM $MgCl_2$, 1.0 mM DTT, pH 7.9), 250 μM dNTPs, 50 nM linear template 1, 50 nM exponential template 1, and the sediment from the previous step. Section B incorporated 1 × Thermopol buffer (20 mmol/L Tris-HCl, 10 mmol/L KCl, 10 mmol/L $(NH_4)_2SO_4$, 2 mmol/L $MgSO_4$, 0.1% Triton X-100, pH 8.8),

Table 1 DNA sequences used in this assay

Name	Sequences (5′-3′)
Enzymatic strand	GGTAAGCCTGGGCCTCTTTCTTTTTAAGAAAGAAC
MB substrate	Biotin-TTTTTT CCACCACATTCAAATTC *AGCTTCTTTCTAATACG**G**CTTACC* TTACGAGGCGGTGGTGG
MB substrate 1	Alexa Fluor 488-CATGCGCGATTCAAATTC *AGCTTCTTTCTAATACG**G**CTTACC* TTACGAGGCGCGCGCATG-BHQ1
MB substrate 2	Alexa Fluor 488-CCACCACATTCAAATTC *AGCTTCTTTCTAATACG**G**CTTACC* TTACGAGGCGGTGGTGG-BHQ1
Trigger 1	CCACCACATTCAAATTC *AGCTTCTTTCTAATACG**G***
ssDNA template 1	AAAAAAAAAAAAAAAAAAAAAAAAAAAAAA |AACAGACTC CCGTATTA GAAAGAAGCT GAATTTGAAT GTGGTGG
Trigger 2	TTTTT TTTTT TTTTT TTTTT TTTTT TTTTT
ssDNA template 2	AAAAAAAAAAAAAAAAAAAAAAAAAAAAAA |AACAGACTC AAAAAAAA AAAAAAAAAAAAAAAAAAAAAA

The italic type, the bold type, the straight-underlined type, and the wave-underlined type are the DNAzymatic substrate domain, DNAzymatic cleavage site, stem domain in the molecular beacon (MB), and the recognition sequence of Nt.Bst NBI, respectively

0.4 U/μL Nt.BstNBI NBI, and 0.008 U/μL Bst DNA polymerase. Sections A and B were freshly prepared on ice, mixed, and transferred to a thermocycler at 55 °C for 10 min.

Preparation of fluorescent copper nanoparticles

Briefly, 15 μL resultant product of as-prepared linear and exponential amplification was mixed with 100 μM $CuSO_4$, 10 × reaction buffer (100 mM MOPS, 1.5 M NaCl, pH 7.6) and ultrapure water to a total volume of 50 μL and magnetically separated at room temperature to collect the supernatant. Then, 2 mM freshly prepared sodium ascorbate was added, and the reaction mixture was incubated at room temperature in the dark for 3 min. Following the reduction of Cu^{2+} ions by sodium ascorbate, the as-prepared copper nanoparticles were generated with fluorescence emission at 625 nm upon the excitation at 340 nm. The morphology of copper nano-shaped particles was observed by high-solution TEM.

Preparation of real water samples

Real tap water was acquired from the local laboratory (Beijing, China). The water samples were conducted with the same protocol as noted above used for the Cu^{2+} detection.

Results and discussion

Principle of the fluorescent colorimetric assay for copper ions

The fluorescent biosensor is presented in Scheme 1. The cascaded cycling amplification includes DNAzymatic cyclic amplification module (part A) and linear/exponential integrated amplification module (part B). The Cu^{2+}-dependent DNAzyme was designed as an intermolecular molecular beacon (MB) DNA nanoswitch, conjugated with magnetic nanoparticles (MNPs). Upon the addition of Cu^{2+}, the enzymatic strand combines with the copper ion to exert cleavage activity to cleave the MB substrate. The released enzyme/Cu^{2+} compound can rebind intact MB substrate to form a new MB DNA nanoswitch, catalyze the cleavage reaction, and proceed with multiple isothermal cycles. Both specific identification/transformation of Cu^{2+} input and the first cyclic amplification are integrated into the DNAzymatic cyclic amplification (Scheme 1A). After magnetic separation, the ssDNA products of the DNAzymatic cyclic amplification hybridize with ssDNA template 1 and extend with Bst DNA polymerase. With the nicking activity of the Nt.Bst NBI nicking enzyme and exfoliation activity of the Bst DNA polymerase, extension and exfoliation are synchronized in the linear amplification. Due to the asymmetry of ssDNA template 1, the T-rich ssDNA products are unable to bind with template 1 but hybridize with ssDNA template 2 instead. The symmetric template 2 contains two copies of the reverse complement of T-rich ssDNA at its 3′ and 5′ termini, separated by the reverse complement of the nicking enzyme recognition site and a required post-cut site spacer. The T-rich ssDNA forms a hybrid with the complement at the 3′ terminal region of the template 2 and serves as a primer for Bst DNA polymerase to synthesize a complement of the template, thereby forming a double-stranded DNA (dsDNA) containing the nicking enzyme recognition site in the middle. Nt.Bst NBI nicking enzyme then nicks the upper strand and releases a copy of T-rich ssDNA that is able to prime another template 2. Bst DNA polymerase elongates the recessed 3′-OH created by the

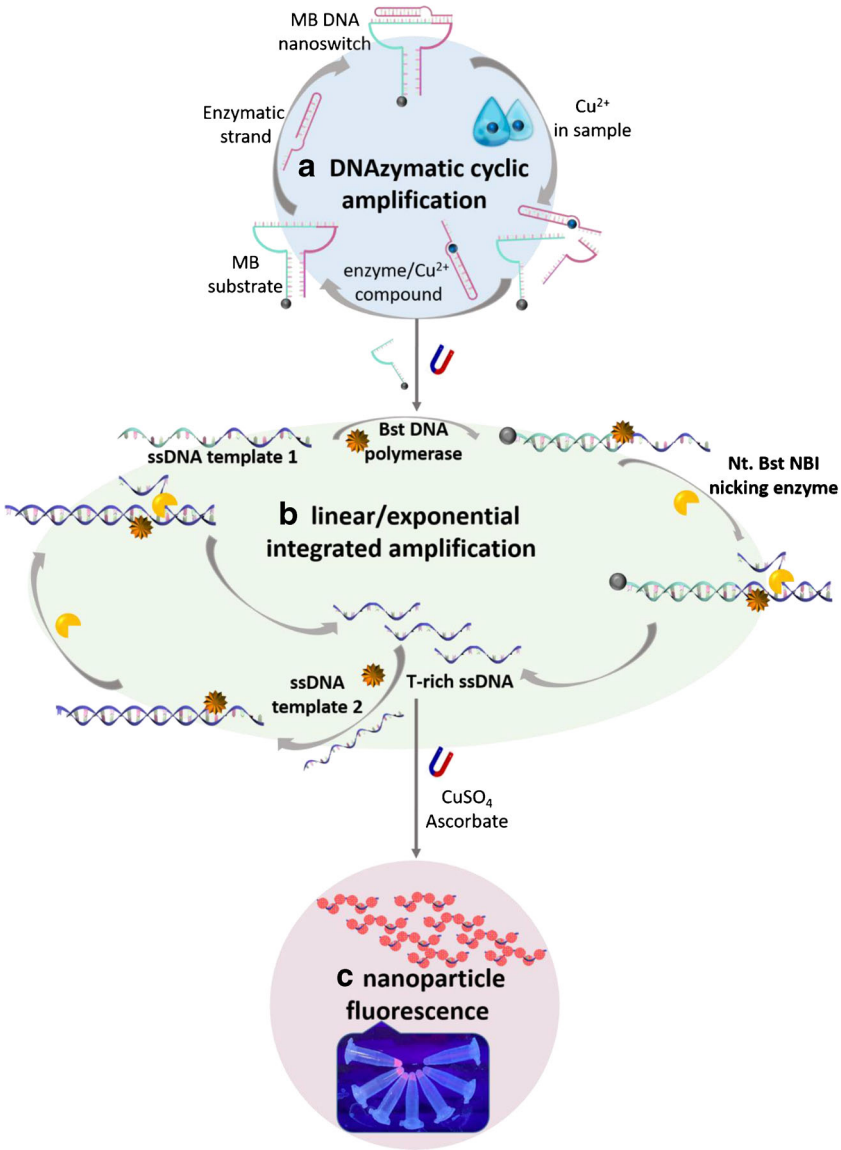

Scheme 1 Schematic illustration of the fluorescent biosensor based on a cascaded cycling amplification and fluorescent copper nanoparticles for Cu^{2+} detection. Section A, identification and transformation from Cu^{2+} input to specific DNA sequences using DNAzymatic cyclic amplification. Section B, the linear/exponential integrated amplification converts specific sequences to unified T-rich scaffolds. Section C, the signal carrier depends on T-rich scaffold-templated fluorescent copper nanoparticles.

departing T-rich ssDNA products and repeats the process. The cycling of replication, nicking, and release reactions results in an exponential replication of T-rich ssDNA with relatively high speed (Scheme 1B). Thereafter, copper ions are activated by the T-rich ssDNA scaffolds of the linear-exponential amplification integrated system and reduced to fluorescent copper nanoparticles as signal carriers to the output detection signal (Scheme 1C).

Feasibility of the cascaded cycling amplification

Characterization and optimization of DNAzymatic cyclic amplification

A fluorescent strategy was projected to represent the DNAzymatic cyclic amplification. As shown in Fig. 1a, the MB substrate was modified with Alexa Flour 488 (AF488), as fluorophore, and Black Hole Quencher (BHQ-1), as quencher, to hybridize with the enzymatic strand for assembly into the MB DNAzyme nanoswitch. The MB DNAzyme was expected to be circularly cleaved with the addition of Cu^{2+}. Firstly, the concentration of the enzymatic strand was kept at 300 nM with the gradual addition of MB substrate in 200 nM increments. As shown in Fig. 1b, the kinetics of the fluorescence intensity showed that the signal increased obviously with each incremental addition; however, when the ratio of MB substrate to enzymatic strand was fourfold, the intensity reached a plateau. Meanwhile, a denaturing polyacrylamide gel electrophoresis (dPAGE) experiment was conducted to demonstrate the cyclic amplification. As shown in Fig. S1A, the MB DNAzyme, comprising 1 μM enzymatic strand and 1, 3, and 6 μM MB substrate, respectively, was characterized in the presence of Cu^{2+}. In 3–8 lanes, the dispersion bands below the band of enzymatic strand became darker and thicker

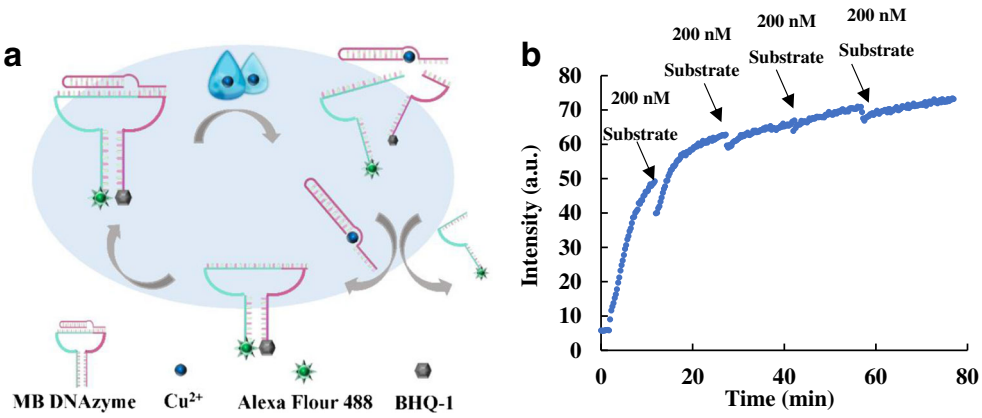

Fig. 1 Characterization of DNAzymatic cyclic amplification. **a** Schematic illustration of the DNAzymatic cyclic amplification is shown. **b** Real-time fluorescent observation of the DNAzymatic cyclic amplification was demonstrated. (Experimental details see Electronic Supp. Material (ESM) 1.2)

with increases in the concentration of MB substrate, thus indicating the generation of more cleavage products as a result of the similar molecular weights of the enzymatic strand and the cleavage products. Consequently, both fluorescence and dPAGE experiments manifested the DNAzymatic cyclic amplification.

Subsequently, MB substrate with different base pairs in stem, cyclic time, and pH in reaction buffer was optimized, respectively. Firstly, MB substrate 1 (MB1) with 8 bp-stem (6GC + 2AT) and MB substrate 2 (MB2) with 7 bp-stem (5GC + 2AT) were compared to obtain the optimal SNR. As shown in Fig. S1B, MB2-composed DNAzyme 2 responded to Cu^{2+} more notably, with 17.4-fold SNR, than did the MB1-composed DNAzyme 1, with 10.2-fold SNR. Secondly, with real-time observation, illustrated in Fig. S1C, the fluorescent signal of MB2-composed DNAzyme 2 rose rapidly to a stabilized level, whereas that of MB1-composed DNAzyme 1 climbed gradually with the addition of 10 μM $CuSO_4$ in 20 min. Thirdly, under different pH conditions, the MB2-composed DNAzyme 2 in pH 7.0 exhibited the optimal fluorescent response (Fig. S1D). Therefore, MB2-composed DNAzyme 2 was circularly cleaved in the pH 7.0 cleaving buffer within 20 min and was applied for the next step.

Characterization and optimization of linear/exponential integrated amplification

To verify the linear/exponential integrated amplification, as shown in Scheme S1, a real-time amplification analysis was conducted with the addition of different concentrations of trigger 1 and trigger 2. To simplify data analysis, the value of cycle threshold (Ct) was used to judge the quantitative detection. Primarily, real-time fluorescent exponential amplification was observed in response to 50 nM template 2 and different concentration trigger 2. As illustrated in the amplification curve (Fig. S2) and the calibration curve (Fig. 2a), the Ct value decreased with the increasing concentration of trigger 2. On the logarithmic scale, the value of Ct represents a linear correlation with 4 orders of magnitude of trigger 2 from 1 pM to 10 nM. The regression equation is Ct = − 8.208c (trigger 2) + 48.192 with a correlation coefficient of 0.9944. Based on the feasibility of exponential amplification, the integrated linear and exponential reaction was demonstrated further. Similarly, the number of Ct descended with the ascending concentrations of trigger 1, thus showing a linear correlation with 3 orders of magnitude of trigger 1 from 1 pM to 1 nM with the regression equation Ct = − 3.6051c (trigger 1) + 25.212 (R^2 = 0.9982), as exhibited in Fig. S3 and Fig. 2b. Compared with the single exponential amplification, the smaller Ct value in the integrated reaction indicates that it is capable of a faster response and higher efficiency and is suitable for modularization to analyze Cu^{2+}.

To improve the detection performance in this integrated module, the dosage ratio of Bst DNA polymerase to Nt.Bst NBI and that of template 1 to template 2 was both optimized. Ct value was also applied to determine the optimal performance for the requirement of rapid analysis. For the enzymatic content (Fig. S4A), the proportion of Nt.Bst NBI was elevated from 1:10 to 1:100, on the fixed 0.008 U/μL Bst DNA polymerase. The Ct value rose with the enhancement of the Nt.Bst NBI ratio. For the templates, the percentage of template 1 was elevated from 10:50 to 100:50, on the settled concentration of 50 nM template 2. As exhibited in Fig. S4B, the Ct value was enhanced with the augmentation of the template 1 proportion. Comprehensively, 1:10 of Bst DNA polymerase to Nt.Bst NBI and 10:50 of template 1 to template 2 were selected as the optimal modularized conditions for the sensitive analysis of Cu^{2+}.

Characterization and optimization of DNA-templated copper nanoparticles

To apply the DNA-templated copper nanoparticles as the signal carrier, T-rich ssDNA (trigger 2) was selected as the model template to manipulate the nanoparticle synthesis. Constant content of Cu^{2+} (100 μM) was deposited on the surface of T-rich scaffolds for nucleation and reduced by sodium ascorbate for fluorescent emission. As indicated in Fig. 3a and S5A,

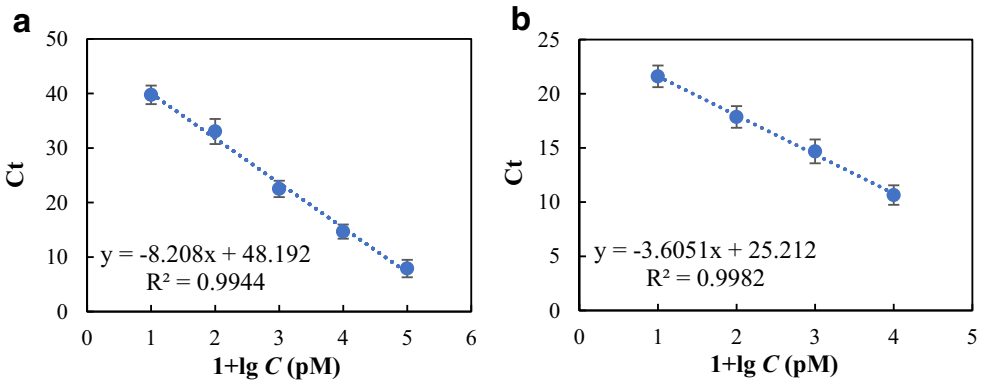

Fig. 2 Characterization of linear/exponential integrated amplification. The calibration curves of **a** the exponential amplification and **b** the integrated linear and exponential reaction were plotted to certify the feasibility of integrated amplification. (Experimental details, see Electronic Supp. Material (ESM) 1.3)

copper nanoparticles transmitted the strongest fluorescence at the wavelength of 625 nm. It is visible to the naked eye under the observation of a portable ultraviolet detector, with the increasing concentrations of T-rich DNA scaffolds. The high-resolution transmission electron microscope (TEM) image in Fig. 3b shows that the T-rich scaffolded copper nanoparticles are monodisperse and spherical. Simultaneously, the lattice distance in the crystal planes of the copper nano-shaped particles was 2.05 Å, in accordance with the (111) plane of fcc phase of metal copper [39], which suggests that the formation of copper nanoparticles correlates with the fluorescence and that the nano-shaped particles is feasible for colorimetric assays.

Subsequently, the feasibility of the cascaded cycling amplification module was demonstrated by means of nanoparticle fluorescence observation after integrated linear/exponential amplification. Trigger 1-initiated integrated amplification/output system and trigger 1-absent integrated amplification/output system were set as the positive sample and the negative control, respectively. The fluorescent kinetic curve in Fig. S5B manifested the rapid nanoparticle synthesis, almost concurrently with the addition of Cu^{2+}, an outstanding fluorescence lifetime of nearly 30 min and excellent SNR of up to 4.5-fold. Analogically, the fluorescence spectra in Fig. S5C also described the differential between the positive sample and the negative control, indicating the feasibility of the universal cascaded cycling amplification module. Furthermore, the amount of sodium ascorbate was explored from 0.5 to 6 mM. Optimally, 2 mM reductant was established for fluorescence intensity, as shown in Fig. S5D.

Analytical performance of the colorimetric assay

Sensitivity

To measure the detectability of our proposed biosensor, the fluorescent response was tested as the increment of Cu^{2+} under optimal conditions. As revealed in Fig. 4a, the fluorescent signal increased with the increasing concentration of copper ions ranging from 10 to10^7 nM. The inset displays the visual image corresponding to the incremental Cu^{2+}. The augment of fluorescent intensity was distinctly proportional to the Cu^{2+} concentration in a wide linear range from 10 to 10^4 nM, with the calibration curve of $Y = 123.3\ \mathrm{Lg}\ C - 11.618$ ($R^2 = 0.9928$, Y is the fluorescent intensity and C is the concentration of copper ion (nM)). The detection limit of 5.6 ± 0.52 nM ($n =$

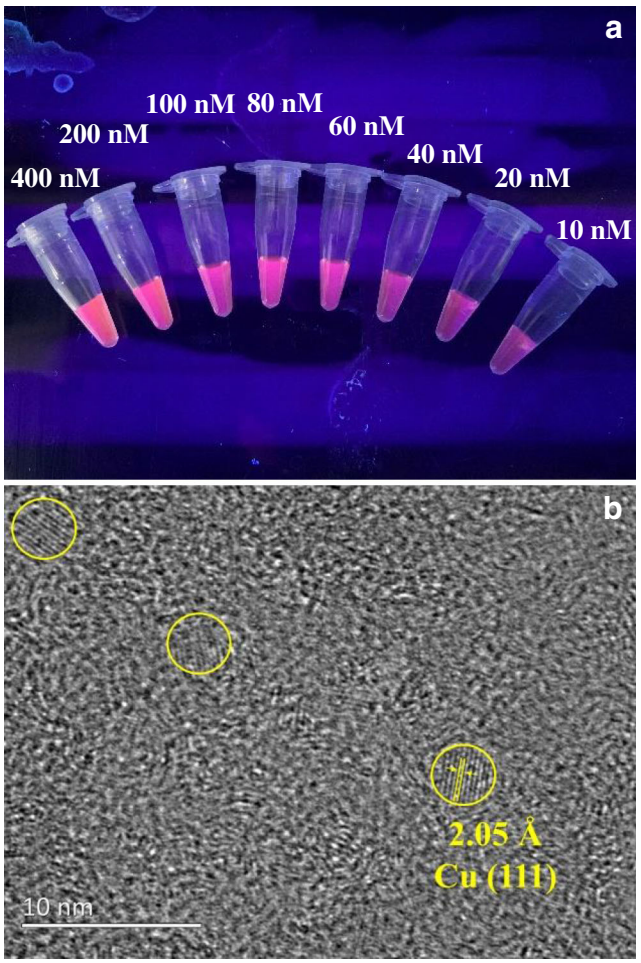

Fig. 3 Characterization of DNA-templated copper nanoparticles. **a** Visual image of copper nanoparticles was acquired under different concentrations of T-rich DNA scaffold. **b** High-resolution TEM image of copper nanoparticles manipulated by poly-T ssDNA. (Experimental details, see Electronic Supp. Material (ESM) 1.4)

3) was estimated according to the 3σ rule (Fluo. = blank average (Fluo.) − 3σ, where σ is the standard deviation of the blank solutions) [40].

Inspiringly, the LOD of this colorimetric method was much lower than the prescribed limits in drinking water set by the World Health Organization (WHO) (2.0 mg/L = 31.25 μM) [41], Environmental Protection Agency (EPA) in the USA (20 μM) [42], and Chinese Ministry of Health (1.0 mg/L = 15.625 μM) [43]. Moreover, the detection limit conformed to the specific standard (2 μg/L = 31.25 nM) in electronic grade water [44]. Besides, our proposed method is comparable with the recent studies (Table 2) and is competent with regard to the ultrasensitive analysis of Cu^{2+}. Several factors possibly support the outstanding sensitivity: (1) Cu^{2+}-responsive DNAzymatic cyclic amplification allowing one target transition into many initiator ssDNA to trigger linear/exponential integrated amplification, (2) the integrated reaction persistently proceeding exponentially, and (3) the highly loaded signal carrier depending on fluorescent copper nanoparticles. Therefore, the cascaded cyclic amplification-lighted nanoparticle fluorescence enables ultrasensitive Cu^{2+} detection. Besides the outstanding performance, our biosensor avoids complicated interface modification that is inherent in the electrochemical or detection. Compared with the current fluorescent and colorimetric methods, copper nanoparticles, used as label-free signal carrier, generated in situ instantaneously instead of pre-modification process. It is economical and user-friendly in the detection.

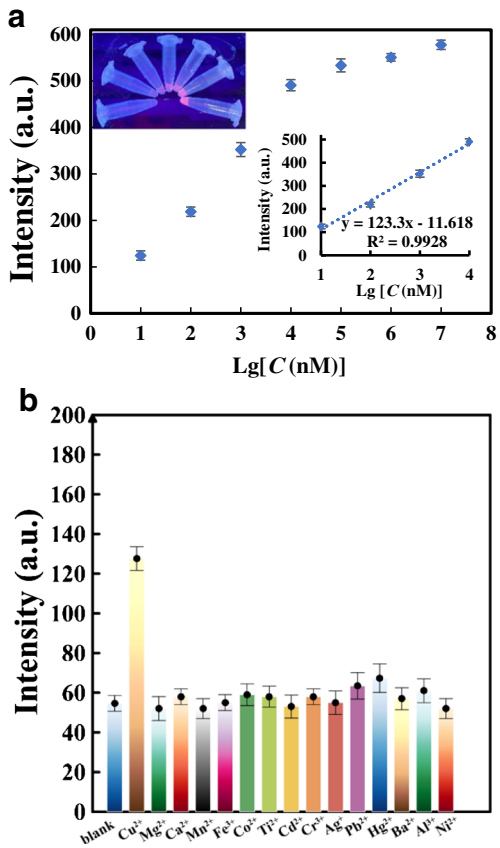

Fig. 4 Analytical performance of proposed colorimetric biosensor. **a** The quantitative detection performance of our fluorescent biosensor. The inset shows the calibration curve and corresponding visual image with respect to Cu^{2+} ranging from 10 to 10^4 nM. (excitation: 340 nm, emission: 625 nm). **b** Specificity of the sensor was explored upon copper ions (10 nM) and fourteen other metal ions (1 mM). (Experimental details, see Electronic Supp. Material (ESM) 1.5)

Selectivity

The selective response of the sensor was subsequently contrasted in different metal ions (1.0 mM), namely, Co^{2+}, Ti^{2+}, Mg^{2+}, Fe^{3+}, Mn^{2+}, Ca^{2+}, Cd^{2+}, Cr^{3+}, Ag^{+}, Pb^{2+}, Hg^{2+}, Ba^{2+}, Al^{3+}, and Ni^{2+}. As illustrated in Fig. 4b, 10 nM copper ions acquired obvious fluorescent response compared with the blank sample, while the other fourteen metal ions presented little difference with the blank, thus demonstrating the extraordinary selectivity of our proposed method. This may be ascribed to the high specificity between Cu^{2+} and DNAzyme, magnetic separation, and excellent SNR of nanoparticle synthesis. Furthermore, when six uniform biosensors were applied to analyze 100 nM Cu^{2+} at the optimum sensing condition, a relative standard deviation (RSD) of 2.36% was achieved (Fig. S6), again illustrating the superior reproducibility of this method.

Detection of Cu^{2+} in tap water

The flexibility of our developed colorimetric biosensor for Cu^{2+} detection was further evaluated using tap water and lake water (Beijing, China) sample. Firstly, samples were tested in triplicate by inductively coupled plasma mass spectrometry (ICP-MS), and the value of determination was taken as the average (421.875 ± 9.84 nM for tap water and 60.37 ± 5.75 μM for lake water, respectively). When the samples were detected by our proposed sample in triplicate, the result was 433.624 ± 7.39 nM and 58.34 ± 4.27 μM, respectively (Table S1). The similar results demonstrated that the biosensor is available for real sample detection.

Conclusion

In conclusion, a cascaded cycling amplification-lighted fluorescent biosensor was developed for the ultrasensitive detection of copper ions. The cascaded cycling amplification includes two modules: (1) The DNAzymatic cyclic amplification unit makes up for the deficiency of Ab failing to respond to metal ions, broadens the range of biomarkers in the field of detection, and achieves the transformation from metal ions to specific DNA sequences. (2) In the linear/exponential integrated amplification unit, the linear reaction connects the

Table 2 Recent Cu^{2+} biosensors developed using Cu^{2+}-dependent cleaving DNAzyme, the type of samples in which the sensors were tested

Detection mode	Sample	LOD	Reference
Fluorescence-based detection	Tap water	500 pM	[45]
Electrochemiluminescent detection	Human hair extract buffer	1 nM	[46]
Electrochemical detection	River water	0.1 aM	[47]
Colorimetric detection	Lake water	8 nM	[48]
Fluorescent detection	Tap water	5.6 nM	This manuscript

previous diverse DNA codes to unified T-rich scaffolds. Afterwards, the T-rich scaffolds combined with a symmetric template for a circuiting feedback mechanism in the exponential reaction. Generally, it meets the increasing need for the ultrasensitive detection.

It establishes the concept of specific signal input-specific cleaved DNAzyme-identical DNA passwords and provides a versatile strategy for different targets. From Pb^{2+}, Cr^{3+}, and Zn^{2+} to *Helicobacter pylori* and *Escherichia coli*, a wide range of targets whose cleaved DNAzyme has been screened can be detected via our proposed concepts. Therefore, the well-designed cascaded cycling amplification offers a solution for one-to-many-type target transformation and an open amplification platform for intelligent response to many kinds of targets.

Meanwhile, fluorescent copper nanoparticles, templated by T-rich scaffolds instantaneously in situ, served as carriers to output detection signals. Compared by labeled signal vehicles, the nano-shaped particles lower the cost, re-amplify signal, and are compatible with the above open platform. Consequently, it provides a user-friendly and economical scheme for FNAs-induced luminescence.

As for limitations, there are two points to specify: (1) The relatively longer detection time. Our scheme offers an ultrasensitive detection scheme, so it is acceptable to consume 40 min per sample for detection. (2) The interference of fluorescent signal. Complex samples, such as blood, serum, cells, marine water, and wastewaters, always display strong background UV absorption and fluorescence. Besides, the excited and emitted UV fluorescence will be screened off by UV absorbers, and this will weaken the signal. As a result, necessary sample pretreatment is crucial.

Funding information This work is supported by the National Science and Technology Major Project (No. 2018ZX08012-001), the National Natural Science Foundation Project of China (No. 31871875), and the Graduate Research and Innovation Project of China Agricultural University (B20183060533).

Compliance with ethical standards

Conflict of interest The authors declare that they have no conflict of interest.

References

1. Xu W (2016) Functional nucleic acids detection in food safety. Springer
2. Wu S, Lin Y, Liu J, Shi W, Yang G, Cheng P (2018) Rapid detection of the biomarkers for carcinoid tumors by a water stable luminescent lanthanide metal-organic framework sensor. Adv Funct Mater 28(17):1707169
3. Esteve-Turrillas FA, Mercader JV, Agulló C, Abad-Somovilla A, Abad-Fuentes A (2018) Highly sensitive monoclonal antibody-based immunoassays for boscalid analysis in strawberries. Food Chem 267:2–9
4. Tian W, Wang L, Lei H, Sun Y, Xiao Z (2018) Antibody production and application for immunoassay development of environmental hormones: a review. Chem Biol Technol Agric 5(1):1–12
5. Sheng W, Chang Q, Shi Y, Duan W, Zhang Y, Wang S (2018) Visual and fluorometric lateral flow immunoassay combined with a dual-functional test mode for rapid determination of tetracycline antibiotics. Microchim Acta 185(9):404
6. Hou T, Zhang L, Sun X, Li F (2016) Biphasic photoelectrochemical sensing strategy based on in situ formation of CdS quantum dots for highly sensitive detection of acetylcholinesterase activity and inhibition. Biosens Bioelectron 75:359–564
7. Wang X, Hou T, Lu T, Li F (2014) Autonomous exonuclease III-assisted isothermal cycling signal amplification: a facile and highly sensitive fluorescence DNA glycosylase activity assay. Anal Chem 86(19):9626–9631
8. Wang X, Gao H, Qi H, Gao Q, Zhang C (2018) Proximity hybridization-regulated immunoassay for cell surface protein and protein-overexpressing cancer cells via electrochemiluminescence. Anal Chem 90(5):3013–3018
9. Xu W, He W, Du Z, Zhu L, Huang K, Lu Y (2019) Functional nucleic acids-nanomaterials: development, properties, and applications. Angew Chem Int Ed. https://doi.org/10.1002/ange.201909927
10. Hu Q, Li H, Wang L, Gu H, Fan C (2018) DNA nanotechnology-enabled drug delivery systems. Chem Rev 119(10):6459–6506
11. Breaker RR, Joyce GF (1994) A DNA enzyme that cleaves RNA. Chem Biol 1(4):223–229
12. Carmi N, Balkhi SR, Breaker RR (1998) Cleaving DNA with DNA. Proc Natl Acad Sci U S A 95(5):2233–2237
13. Ali MM, Wolfe M, Tram K, Gu J, Filipe CD, Li Y (2019) A DNAzyme-based colorimetric paper sensor for Helicobacter pylori. Angew Chem Int Ed 58(29):9907–9911
14. Lake RJ, Yang Z, Zhang J, Lu Y (2019) DNAzymes as activity-based sensors for metal ions: recent applications, demonstrated advantages, current challenges, and future directions. Acc Chem Res 52(12):3275–3286
15. Zhu L, Li G, Shao X, Huang K, Luo Y, Xu W (2020) A colorimetric zinc(II) assay based on the use of hairpin DNAzyme recycling and a hemin/G-quadruplex lighted DNA nanoladder. Microchim Acta 187(1):26

16. Tian J, Huang K, Luo Y, Zhu L, Xu Y, Xu W (2018) Visual single cell detection of dual-pathogens based on multiplex super PCR (MS-PCR) and asymmetric tailing HCR (AT-HCR). Sensors Actuators B Chem 260:870–876
17. Li S, Zhang Y, Tian J, Xu W (2020) Luminescent DNAzyme and univerferesal blocking linker super polymerase chain reaction visual biosensor for the detection of Salmonella. Food Chem 324: 126859
18. Tian J, Chu H, Zhang Y, Li K, Tian H, Zhang X, Xu W (2019) TiO_2 nanoparticle-enhanced linker recombinant strand displacement amplification (LRSDA) for universal label-free visual bioassays. ACS Appl Mater Interfaces 11(50):46504–46514
19. Gao W, Tian J, Huang K, Yang Z, Xu W, Luo Y (2019) Ultrafast, universal and visual screening of dual genetically modified elements based on dual super PCR and a lateral flow biosensor. Food Chem 279:246–251
20. Pinheiro AV, Han D, Shih WM, Yan H (2011) Challenges and opportunities for structural DNA nanotechnology. Nat Nanotechnol 6(12):763–772
21. Zhang Z, Liu T, Wang S, Ma J, Zhou T, Wang F (2019) DNA-templated gold nanocluster as a novel fluorometric sensor for glutathione determination. J Photochem Photobiol A 370:89–93
22. Chang J, Wang X, Wang J, Li H, Li F (2019) Nucleic acid-functionalized metal-organic framework-based homogeneous electrochemical biosensor for simultaneous detection of multiple tumor biomarkers. Anal Chem 91(5):3604–3610
23. Feng Y, Shao X, Huang K, Tian J, Mei X, Luo Y, Xu W (2018) Mercury nanoladders: a new method for DNA amplification, signal identification and their application in the detection of Hg (II) ions. Chem Commun 54(58):8036–8039
24. Kim S, Kim JH, Kwon WY, Hwang SH, Cha BS, Kim JM (2019) Synthesis of DNA-templated copper nanoparticles with enhanced fluorescence stability for cellular imaging. Microchim Acta 186(7): 479
25. Yang H, Xu W, Zhou Y (2019) Signal amplification in immunoassays by using noble metal nanoparticles: a review. Microchim Acta 186(12):859
26. Rotaru A, Dutta S, Jentzsch E, Gothelf K, Mokhir A (2010) Selective dsDNA-templated formation of copper nanoparticles in solution. Angew Chem Int Ed 49(33):5665–5667
27. Qing Z, He X, He D, Wang K, Xu F, Qing T (2013) Poly (thymine)-templated selective formation of fluorescent copper nanoparticles. Angew Chem Int Ed 52(37):9719–9722
28. Li X, Du Z, Lin S, Tian J, Tian H, Xu W (2020) ExoIII and TdT dependent isothermal amplification (ETDA) colorimetric biosensor for ultra-sensitive detection of Hg^{2+}. Food Chem 316:126303
29. Li S, Zhu L, Li G, Du Z, Tian J, Luo Y, Xu W (2019) A "turn-off" ultra-sensitive fluorescent quantitative biosensor driven by zinc ion DNAzyme. Sensors Actuators B Chem 285:173–178
30. Zhu L, Miao M, Shao X, Du Z, Huang K, Luo Y, Xu W (2019) A universal electrochemical biosensor using nick-HCR nanostructure as molecular gate of nanochannel for detecting chromium(III) ions and microRNA. Anal Chem 91(23):14992–14499
31. Wang Z, Yu X, Li F, Kong F, Lv W, Fan D (2017) Preparation of boron-doped carbon dots for fluorometric determination of Pb (II), Cu (II) and pyrophosphate ions. Microchim Acta 184(12):4775–4783
32. Xu W, Zhou X, Gao J, Xue S, Zhao J (2017) Label-free and enzyme-free strategy for sensitive electrochemical lead aptasensor by using metal-organic frameworks loaded with AgPt nanoparticles as signal probes and electrocatalytic enhancers. Electrochim Acta 251:25–31
33. Yun W, Du X, Liao J, Sang G, Chen L, Li N (2018) Three-way DNA junction based platform for ultra-sensitive fluorometric detection of multiple metal ions as exemplified for Cu (II), Mg (II) and Pb (II). Microchim Acta 185(6):306
34. Liao Y, Guo S, Hua X, Yuan R, Xu W (2020) Autocatalytic replicated Mg^{2+}-ligation DNAzyme as robust biocatalyst for sensitive, label-free and enzyme-free electrochemical biosensing of protein. Sensors Actuators B Chem 310:127862
35. Xu W, Zhu L, Shao X, Huang K, Luo Y (2018) An electrochemical biosensor based on nucleic acids enzyme and nanochannels for detecting copper (II) ion. Biosens Bioelectron 120:168–174
36. Ibrahim I, Lim HN, Huang NM (2019) Cellulose acetate beads modified with cadmium sulfide and methylene blue for adsorbent-assisted photoelectrochemical detection of copper (II) ions. Microchim Acta 186(7):452
37. Huang X, Jiang H, Li Y, Sang L, Zhou H, Shahzad SA (2017) Synthesis of silica nanoparticles doped with $[Ru(bpy)_3]^{2+}$ and decorated with silver nanoclusters for the ratiometric photoluminescent determination and intracellular imaging of Cu (II) ions. Microchim Acta 184(7):2325–2331
38. Georgopoulos P, Roy A, Yononelioy MJ, Opiekun RE, Lioy PJ (2001) Environmental copper: its dynamics and human exposure issues. J Toxicol Environ Health B 4(4):341–394
39. Vilar-Vidal N, Blanco MC, LóPez-Quintela MA, Rivas J, Serra C (2010) Electrochemical synthesis of very stable photoluminescent copper clusters†. J Phys Chem C 114(38):15924–15930
40. Macdougall D, Crummett W (1980) Guidelines for data acquisition and data quality evaluation in environmental chemistry. Anal Chem 52(14):2242–2249
41. World Health Organization Staff (2004) Guidelines for drinking-water quality [M]. World Health Organization: Vol. 1
42. United States Environmental Protection Agency. Office of Wastewater Management. Municipal Support Division, National Risk Management Research Laboratory (US). Technology Transfer, Support Division (2004) Guidelines for water reuse[M]. US Environmental Protection Agency
43. Ministry of Health of the People's Republic of China (2006) Standards for drinking water quality. National Standards: GB 5749
44. General Administration of Quality Supervision, Inspection and Quarantine of the People's Republic of China, China National standardizing committee (2013) Electronic grade water. National Standards: GB/T 114461
45. Chen Y, Chen L, Ou Y (2016) DNAzyme-based biosensor for Cu^{2+} ion by combining hybridization chain reaction with fluorescence resonance energy transfer technique. Talanta 155:245–249
46. Lei YM, Zhao M, Wang A (2016) Electrochemiluminescence of supramolecular nanorods and their application in the "on-off-on" detection of copper ions. Chem Eur J 22(24):8207–8214
47. Tian R, Chen X, Liu D (2016) A sensitive biosensor for determination of Cu^{2+} by one-step electrodeposition. Electroanal 28(7): 1617–1624
48. Xu W, Tian J, Luo Y (2017) A rapid and visual turn-off sensor for detecting copper (II) ion based on DNAzyme coupled with HCR-based HRP concatemers. Sci Rep 7:43362